Ricerca Sistema Elettrico	Sigla di identificazione	Distrib.	Pag.	di
	ADPFISS - LP2 - 075	L	1	28

Titolo

Report sull'accoppiamento di codici CFD e codici di sistema

Ente emittente **UNIPI-GRNSPG (CIRTEN)**

PAGINA DI GUARDIA

Descrittori

Tipologia del documento: **Rapporto Tecnico**

Collocazione contrattuale: Accordo di programma ENEA-MSE su sicurezza nucleare e reattori di IV generazione

Argomenti trattati: Tecnologia dei metalli liquidi
Generation IV reactors
Calcolo Parallelo

Sommario

This report describes the work performed by the Gruppo di Ricerca Nucleare di San Piero a Grado (GRNSPG) of the University of Pisa (as member of CIRTEN consortium) in the frame of the "Accordo di Programma MSE-ENEA sulla Ricerca di Sistema Elettrico - Piano Annuale di Realizzazione 2013". The objective of the performed activity was to further contribute to the qualification and improvement of the CFD/system-code coupling tool that had previously been developed in the framework of PAR 2011 and PAR 2012 by the same working group. The scientific and technological relevance of such contribution relies on the fact that the availability of qualified thermal-hydraulic analysis tools and methodologies, which combine multi-scale simulation capabilities, allows a more accurate analysis of nuclear reactor cooling systems (to support both design and safety assessment) in those cases featuring a close interaction between system-scale phenomena (e.g. the natural circulation in a nuclear reactor cooling loop) and local and inherently three-dimensional phenomena (e.g. the heat transfer between coolant and fuel rods, etc.).

Note

Rapporto emesso da UNIPI-GRNSPG (CIRTEN).

Autori:
F. Moretti, M. Lanfredini, L. Mengali, F. D'Auria

Copia n. **In carico a:**

REV.	DESCRIZIONE	DATA		CONVALIDA	VISTO	APPROVAZIONE
2			NOME			
			FIRMA			
1			NOME			
			FIRMA			
0	EMISSIONE	24/09/2014	NOME	Mariano Tarantino	NA	Mariano Tarantino
			FIRMA			

CIRTEN

Consorzio **I**nteruniversitario per la **R**icerca **TE**cnologica **N**ucleare

UNIVERSITY OF PISA

S. PIERO A GRADO NUCLEAR RESEARCH GROUP

Report sull'accoppiamento di codici CFD e codici di sistema

Autori

F. Moretti

M. Lanfredini

L. Mengali

F. D'Auria

CERSE-UNIPI RL 1511/2014

PISA, 22 Settembre 2014

Lavoro svolto in esecuzione dell'Attività LP2.c.1_d
AdP MSE-ENEA sulla Ricerca di Sistema Elettrico - Piano Annuale di Realizzazione 2013
Progetto B.3.1 "Sviluppo competenze scientifiche nel campo della sicurezza nucleare e collaborazione ai programmi internazionali per il nucleare di IV generazione"

List of Contents

List of Figures

1 Introduction

This report describes the work performed by the Gruppo di Ricerca Nucleare di San Piero a Grado (GRNSPG) of the University of Pisa (as member of CIRTEN consortium) in the frame of the "Accordo di Programma MSE-ENEA sulla Ricerca di Sistema Elettrico - Piano Annuale di Realizzazione 2013" (Ref. [1]).

In particular, this report constitutes the deliverable LP2.c.1_d of the corresponding activity scheduled in "Linea Progettuale 2" of Project B.3.1.

The objective of the performed activity was to further contribute to the qualification and improvement of the CFD/system-code coupling tool that had previously been developed in the framework of PAR 2011 and PAR 2012 by the same working group (Refs. [2] and [3]).

The scientific and technological relevance of such contribution relies on the fact that the availability of qualified thermal-hydraulic analysis tools and methodologies, which combine multi-scale simulation capabilities, allows a more accurate analysis of nuclear reactor cooling systems (to support both design and safety assessment) in those cases featuring a close interaction between system-scale phenomena (e.g. the natural circulation in a nuclear reactor cooling loop) and local and inherently three-dimensional phenomena (e.g. the heat transfer between coolant and fuel rods, etc.)

The carried out activity focused on the simulation, for coupled-code benchmarking purposes, of an experiment that could both offer measured data for comparison and be of practical interest in relation to liquid metal coolant technology. For such purpose reference was made to one of the experiments that had been performed in the past on the NACIE test facility (ENEA-Brasimone) in the framework of an experimental campaign on natural and/or assisted circulation of a lead-bismuth eutectic alloy in a closed loop (the natural circulation being driven by an electrically heated fuel pin simulator and the assisted circulation being induced by Argon gas injection).

The tools used for the activity are:

- the thermal-hydraulic system code RELAP5-3D v.4.1.3 (in short: RELAP);
- the CFD code ANSYS CFX v15.0 (in short: CFX);
- the two-way coupling tool previously developed, which includes various routines and a graphical user interface.

The work is structured according to the following main steps:

1. Stand-alone 1D simulation of one NACIE experiment by RELAP.
    - This step required the development of a 1D nodalization of the loop, and its adjustment through an iterative process involving analysis, comparison and parameter tuning to fit the experimental data.
2. Development of a CFD simulation model of the part of the loop containing the fuel pin simulator, where the "local" phenomena of interest (i.e. the coolant-pin heat transfer) take place.
    - The CFD simulation model includes: geometrical modeling of the computational domain; generation of computational meshes (with different refinements); set-up of a CFX input (model selection, numerical parameters, etc.).
    - The CFD model is meant to be coupled to the system code one at a later stage.
3. Set-up of the two-way coupling between RELAP and CFX.
    - This step required modifications to the RELAP nodalization (so as to remove the part corresponding to the fuel pin simulator, and to create the interfaces for the on-line two-way data transfer between the two computational domains during the coupled calculation), some adjustments to the coupling tool and the graphical interface, and several simulation tests.
4. Running the coupled-code simulation; results analysis and comparison.

The results obtained from the coupled calculation are consistent with those obtained from the 1D standalone calculation, which constitutes a further confirmation of the validity of the coupling tool and of its applicability to the thermal-hydraulic analysis of liquid metal coolant systems.

The data from NACIE experiments is not CFD-grade and thus cannot be used for validation of the CFD model capabilities (which is out of the scope of the activity and for which, on the other hand, an extensive literature exists).

2 Description of NACIE Test Facility

An exhaustive description of the NACIE test facility can be found in Ref. [4]. Brief information about the most relevant features is provided hereafter.

Basically, the facility consists of a rectangular loop, 7.5 m high and 1 m wide, with a heat source on the bottom of one side and a heat sink on the top of the other side, in order to allow the establishment of a natural circulation flow (see the sketch in Figure 1). Most of the loop piping is obtained from 2.5 inch – schedule 40 stainless steel pipes. The loop is filled with approximately one ton of LBE.

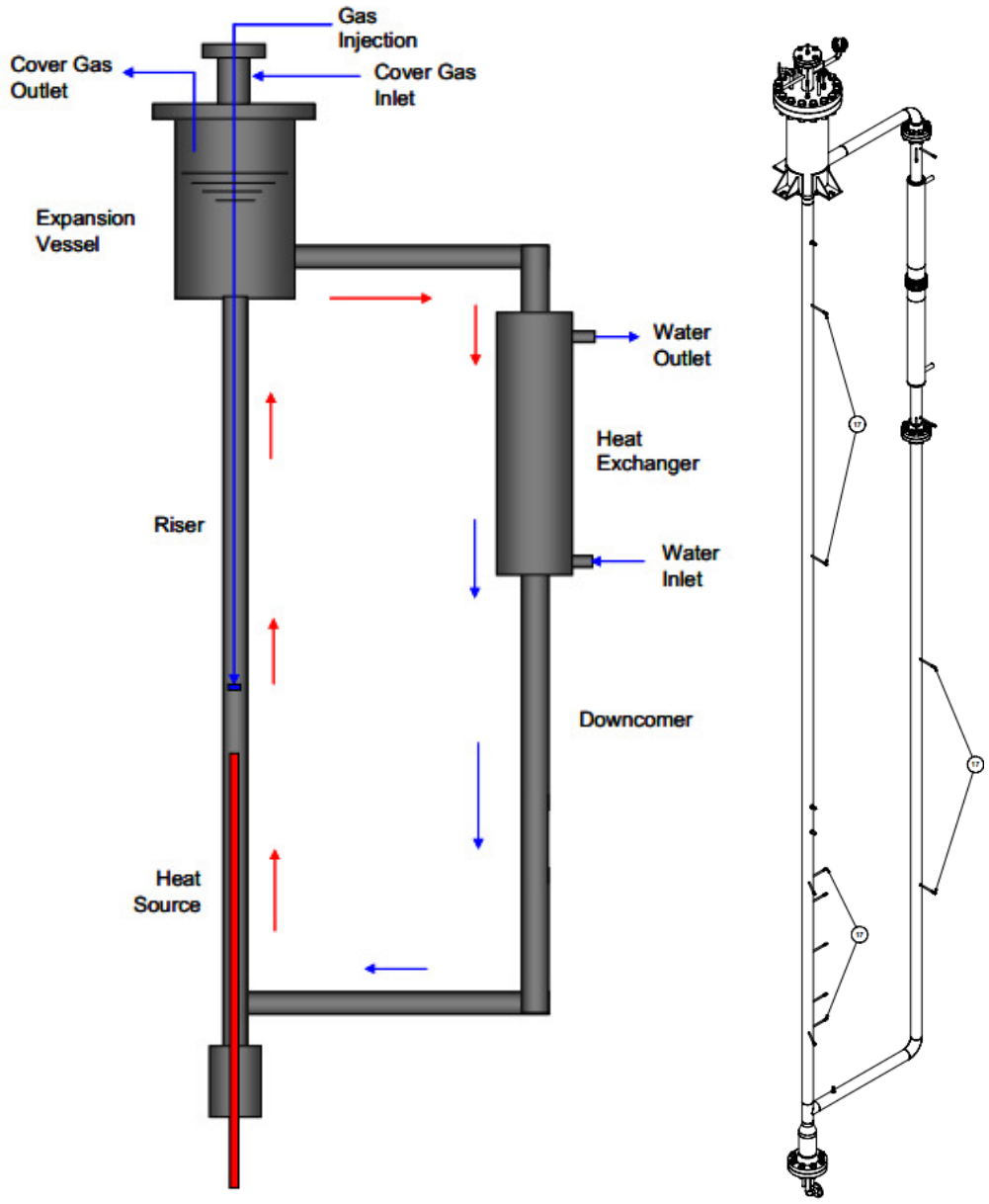

Figure 1: Sketch (left) and 3D model (right) of NACIE loop (Ref. [4]).

A fuel pin simulator (FPS) constitutes the heat source; it includes two electrically heated rods and two dummy rods, the active length being 0.85 m. Two spacer grids are placed at mid height and at the top of the bundle respectively (see Figure 2).

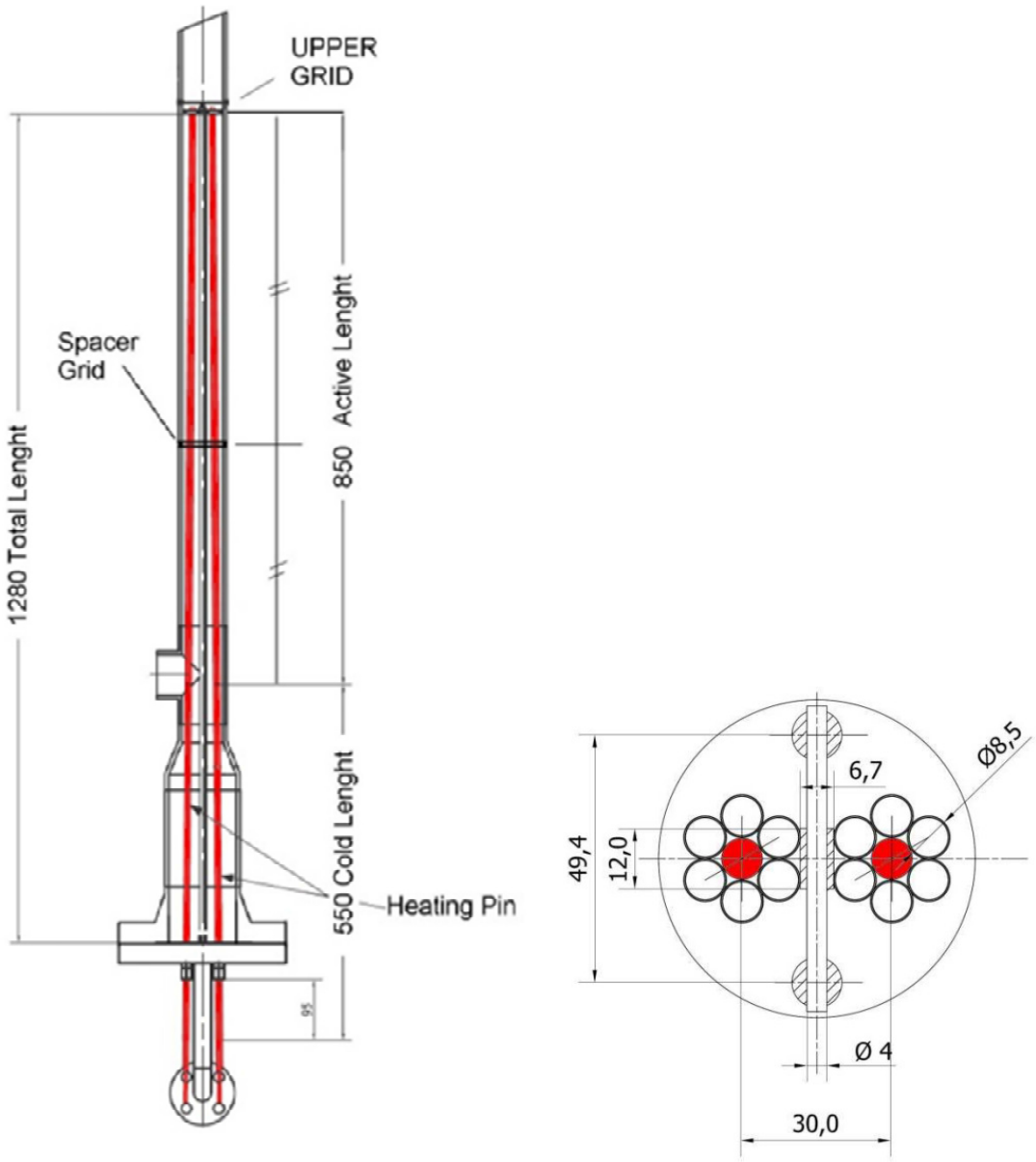

Figure 2 – Fuel pin simulator (Ref. [4]).

The top of the rising pipe enters into an expansion vessel (Figure 3), partly filled with LBE, under an atmosphere of Argon. The vessel compensates volume variations of the LBE inventory, associated with average temperature variations. Moreover, in gas-lift experiments, it collects the Argon that comes up from the riser and keeps it from finding its way through the rest of the circuit.

A small tube (d = 8 mm) enters from the top of the expansion vessel, coaxial with the riser, and ends somewhere above the FPS. Such tube is used in gas-lifted circulation experiments to inject Argon gas.

A heat exchanger (Figure 4) is found on the top part of the downcomer. It is constituted by a 2.5 inch pipe (the same type as the main piping), by a larger (4") coaxial pipe (which represents a sort of "shell"), and by an intermediate tube (3", 2.11 mm thick). The annular region between the 2.5" pipe and the intermediate tube is filled with steel powder, which allows a sort of structural decoupling between the main pipe and the shell (so as to reduce the thermal stresses induced by the large temperature differences) while keeping a reasonably low thermal resistance. An inlet and an outlet nozzle connect the shell to a cooling water circuit;

the water flows in the annular region between the intermediate tube and the shell; the flow is counter-current with respect to the LBE flow. The water is in turn cooled by a fan cooler.

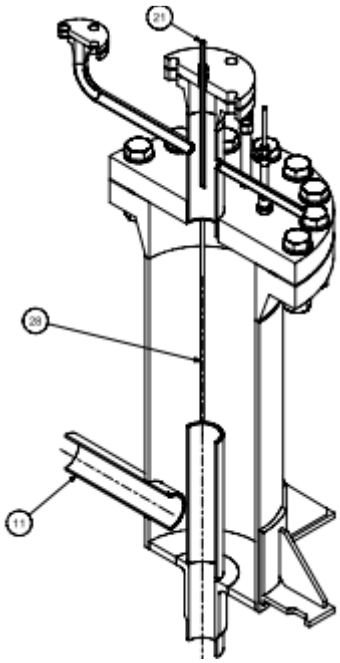

Figure 3 – Expansion vessel (Ref. [4]).

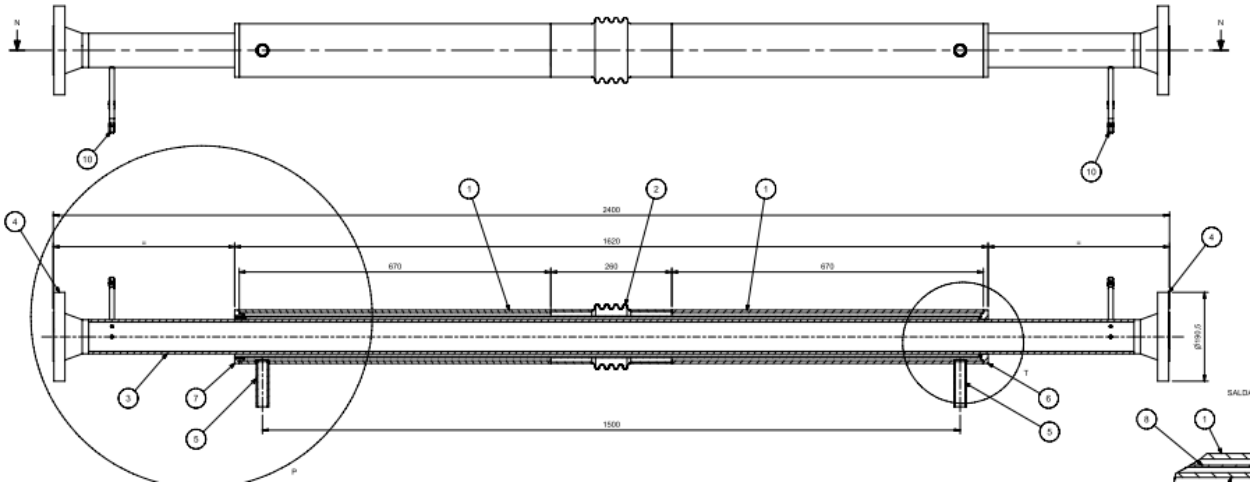

Figure 4 – Heat exchanger (Ref. [4]).

The whole loop is insulated by mineral wool; information on the thickness and the thermal properties of the insulating material is currently unavailable to the Authors.

Electrically heating wires wrap the entire loop, and provide the necessary power to keep the LBE temperature close to 300 °C before and after the conduction of the experiments. No further information is available on the heating wires.

During the experimental campaign that is made reference to, ten tests were carried out, the main features of which are summarized in Table 1.

The various tests differ by the following parameters:

- Average temperature range of LBE (either 200-250 °C or 300-350 °C)
- Power supplied by the FPS (0, 3.5, 9.5 and 21.5 W)
- Heat sink (either used or not)
- Argon injection flow rate (three cases being pure natural circulation tests, i.e. involving no gas injection)
- Transition from natural circulation to gas lifted circulation, and/or viceversa

The tests selected as a benchmark case for the present study is no. 301 (full power, i.e. 21.5 kW, reached with a 5 min ramp; heat sink active; no gas lift; averaged temperature in the range 300-350 °C; no transition observed).

Table 1 – Experimental campaign (Ref. [4]).

ID	T_{av} [°C]	Power %	Power [kW]	Ramp t [min]	Heat Sink	Glift [Nl/min]	Transition NC to GLC	Transition GLC to NC
201	200-250	50	9.5	5	YES	0	NO	NO
203	200-250	50	9.5	5	YES	5	NO	YES
204	200-250	50	9.5	5	YES	2,4,5,6,8, 10,6,5,4,2	YES	NO
206	200-250	0	0	-	NO	2,4,5,6,8, 10,6,5,4,3	NO	NO
301	300-350	100	21.5	5	YES	0	NO	NO
303	300-350	100	21.5	5	YES	5	NO	YES
304	300-350	100	21.5	5	YES	2,4,5,6,8, 10,6,5,4,2	YES	NO
305	300-350	50	9.5	5	YES	0	NO	NO
306	300-350	0	0	-	NO	2,4,5,6,8, 10,6,5,4,2	NO	NO
406	350-360	25	3.5	5	NO	2,4,5,6,8, 10,6,5,4,2	NO	NO

Data from the following instrumentation is available:

- F101 measured gas flowrate [Nl/min]
- IR2 rod bundle current supplied [A]
- M201 pump velocity [rpm]
- M202 air-cooler velocity [rpm]
- MP101 LBE mass flowrate [kg/s]
- MP102 water mass flowrate (secondary side) [kg/s]
- PR2 rod bundle power [kW]
- T101 to T109 termocouples along the loop (see P&I)
- T110 argon temperature
- T201 HX water inlet temperature
- T202 HX water outlet temperature
- VR2 rod bundle tension [V]

The following observations about the instrumentation and the related available data should be made:

- The LBE flow rate (MP101) was measured by an electromagnetic induction flow meter, which showed poor accuracy for the relatively low flow rates developing in the selected test. The related data cannot be used for quantitative comparison, and one has to rely on thermal balance considerations.
- The water flow rate and the pumps speed data are somewhat inconsistent with each other and with the temperature information; one has to carefully analyze the data and possibly apply corrections, with the help of thermal balance considerations.
- LBE temperature measurements were performed at several locations along the loop (information on the exact positions being not available to the Authors). Some uncertainty may affect those temperature data due to the expected non-uniform temperature distribution over the pipe cross sections, especially in the FPS region.
- Inlet and outlet water temperature are also measured; the latter is to be used with care because when the water circulation starts, intense water evaporation occurs, and the measured temperature may at such stage refer to a two-phase mixture or even to dry steam.

During test no. 301 the FPS is powered starting from t = 9320 s (the target power level being reached at about 9600 s), until approximately 27000 s. During such interval the power keeps approximately constant, with an average of 21.9 kW (see Figure 5, green curve, right axis). This data can directly be used as boundary condition for the numerical analyses.

The same figure also shows the flow rate measured by the inductive meter (blue curve), and the flow rate calculated from a thermal balance (using the FPS power and the inlet and outlet LBE temperatures). The discrepancy is noticeable. It has to be noticed that the thermal balance is intended for stationary conditions, and thus does not account for the thermal inertias affecting the materials during a transient.

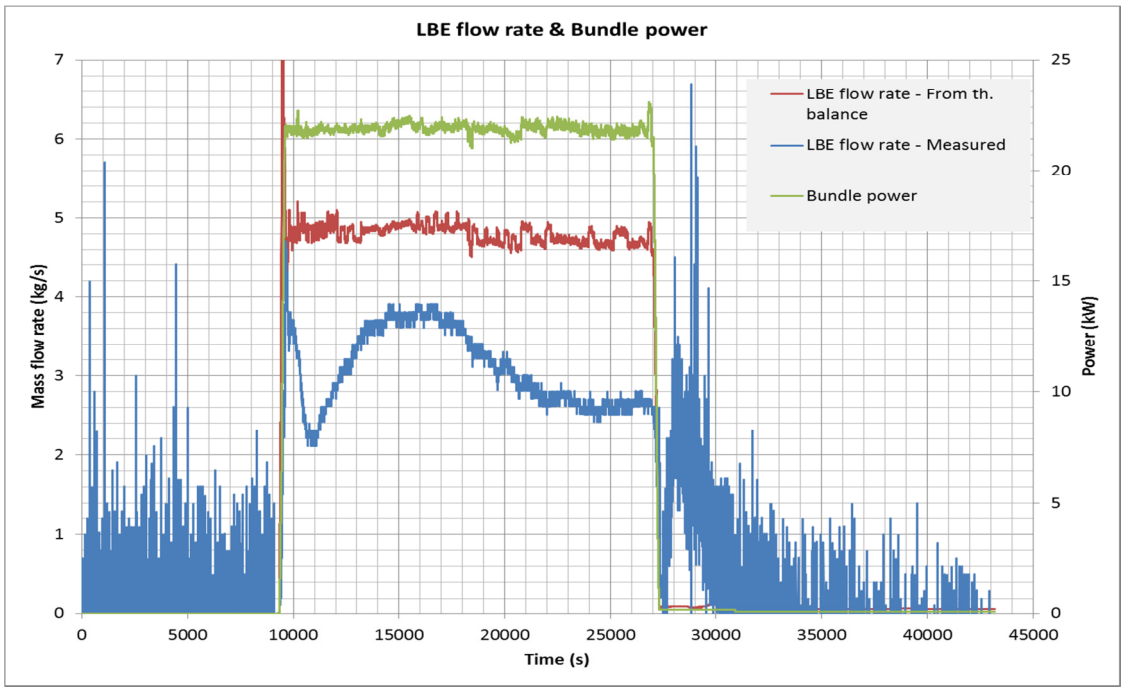

Figure 5 – FPS power and LBE flow rate during test 301.

Figure 6 show the temperatures of the LBE measured at several locations. One can notice that the initial temperatures do not coincide (which indicates some non-uniformity in the temperature distribution, and possibly the presence of colder plugs). On the average the initial temperature is about 290 °C. For roughly

one hour after the start of the power supply all the temperatures increase, until they reach a maximum; then they gradually decrease during the following three hours until quasi-stationary conditions are achieved. The temperature difference between the hot and the cold part of the loop keeps almost constant during the entire transient (about 31-32 °C), hence the constant "calculated-from-balance" flow rate trend seen above.

Two temperatures can be used in particular for comparison purposes: T109 (located somewhere between the HX and the FPS) and T105 (located somewhere above the FPS).

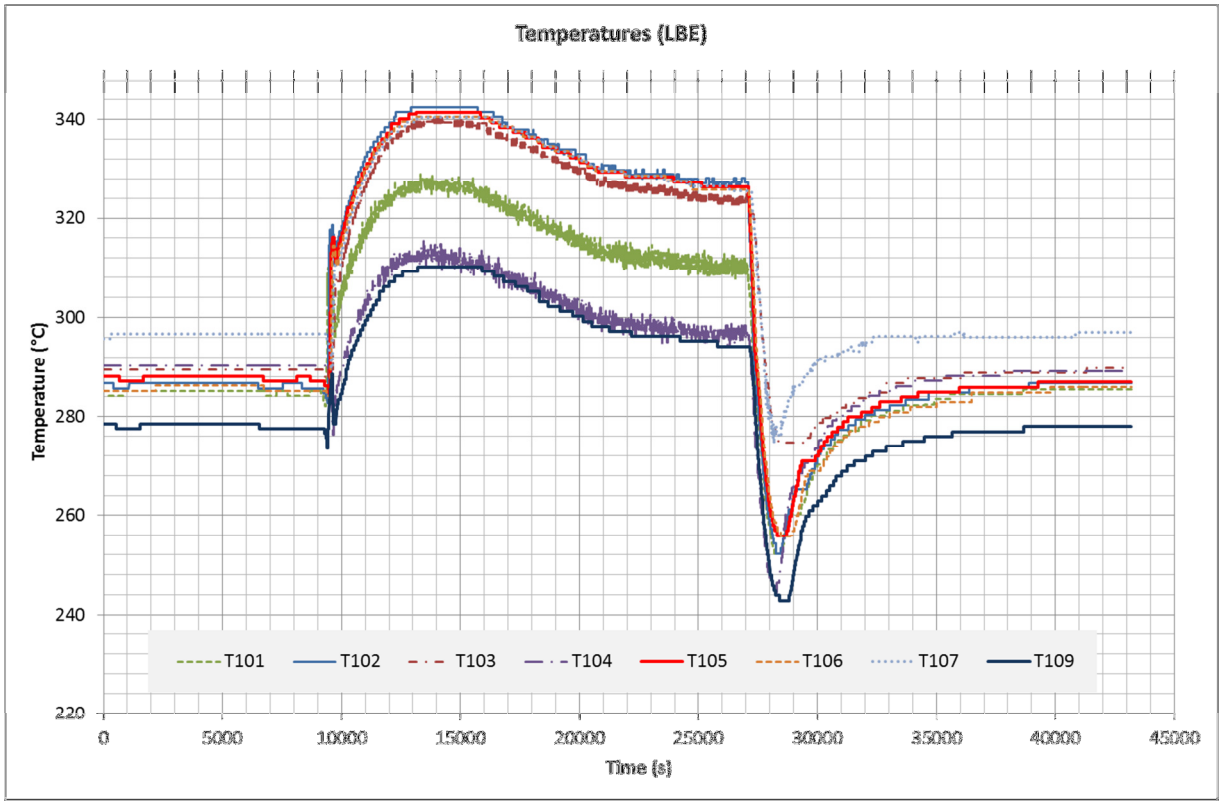

Figure 6 – LBE temperatures during test 301.

The cooling water temperatures (inlet and outlet of the heat exchanger) are shown in Figure 7. The measurements before the start of power supply are not meaningful because no water is flowing through the heat exchanger. After the power start, the operators first let little water flow and then switched on the circulation pump (see Figure 8). The temperature difference between outlet and inlet water takes about one hour to reach a stationary level (about 30.7 °C), which keeps between 15000 s and 22200 s; then the outlet temperature shows a jump that brings the temperature difference to 40.7 °C. The jump corresponds to a step decrease in the pump speed, and thus a decrease of the water flow rate (which indicates that the flow rate shown in Figure 8 is clearly wrong).

The water inlet temperature can be used as a boundary condition for code calculations.

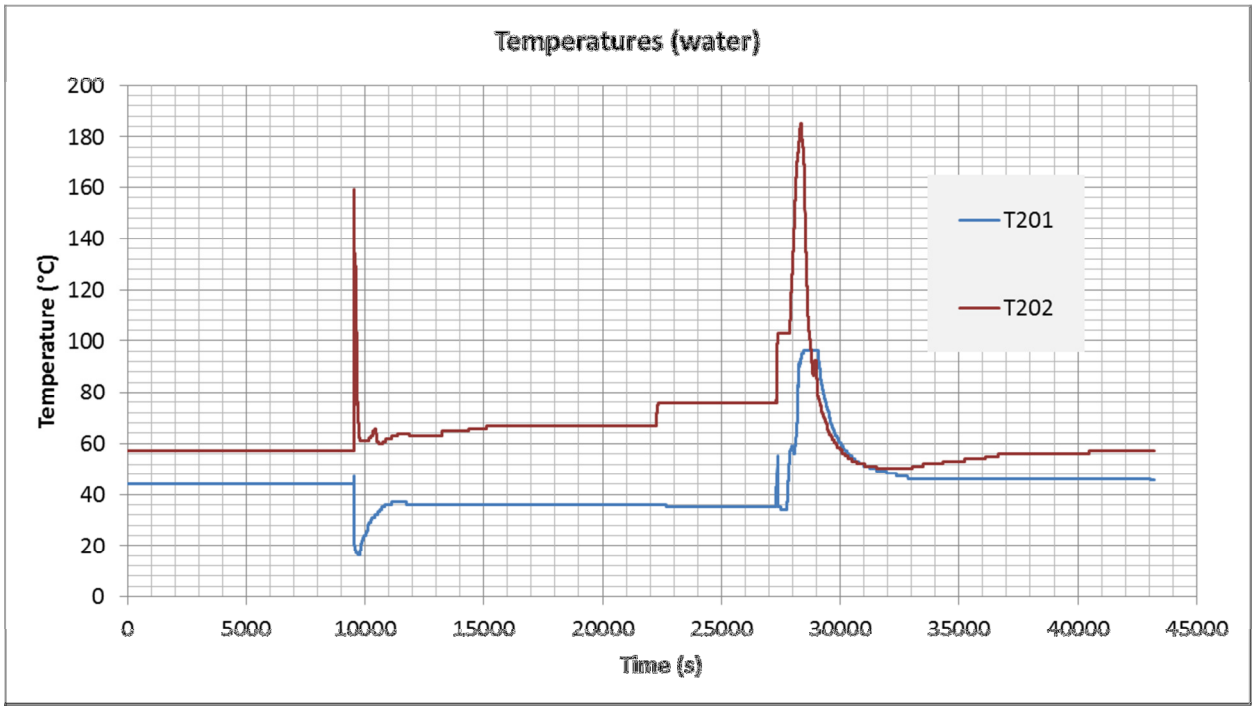

Figure 7 – Water temperature (at heat exchanger inlet and outlet) during test 301.

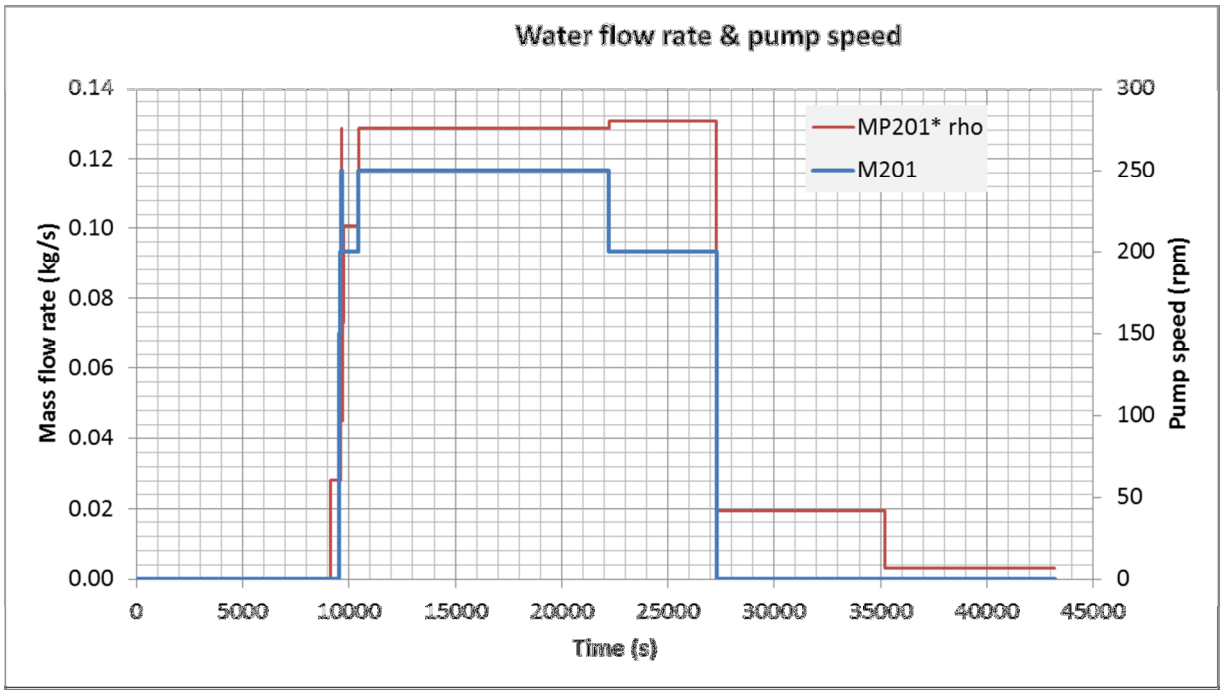

Figure 8 – Water flow rate and pump speed during test 301.

3 RELAP5-3D Stand-alone Modelling

3.1 Nodalization

The RELAP standalone model consists of a 1D nodalization, capable of simulating the natural/assisted circulation experiments, including the definition of all geometrical, physical and operating parameters that affect the system behaviour during the tests.

A sketch of the developed nodalization is shown in Figure 9. The following hydraulic components are used for the LBE loop:

- Branch 110: connection between the horizontal feeding line and the riser
- Pipe 120: part of the riser that contains the heating section (which hosts the FPS), plus some extra length
- Pipe 125: next part of the riser up to the Argon injection location
- Branch 130: Argon injection
- Pipe 140: part of the riser between the Argon injection and the expansion vessel (actually the pipe enters inside the vessel)
- Branch 145: part of the expansion vessel above the top of the riser
- Pipe 150: top part of the expansion vessel
- Time-dependent volume 160: Argon atmosphere above the expansion vessel
- Pipe 170: annular zone in the bottom of the expansion tank
- Pipe 180: horizontal pipe connecting the expansion tank to the downcomer
- Pipe 190: top part of the downcomer, upstream of the heat exchanger
- Pipe 200: heat exchanger (LBE side)
- Pipe 210: downcomer (downstream of the heat exchanger)
- Pipe 220: horizontal pipe connection the downcomer to the heating section

Some single junction connections are used to connect components where branch connections are not available.

The time-dependent volume 132 and the time-dependent junction 135 have been defined (but not enabled) for possible application to assisted circulation cases.

The water cooling circuit is constituted by the following components:

- Time-dependent volume 300: to provide water inlet temperature boundary conditions
- Time-dependent junction 305: to provide water flow rate boundary conditions
- Annulus 310: shell side of the heat exchanger
- Branch 315: heat exchange outlet (to be used as an outlet temperature “probe”)
- Time-dependent volume 320: to provide pressure boundary conditions

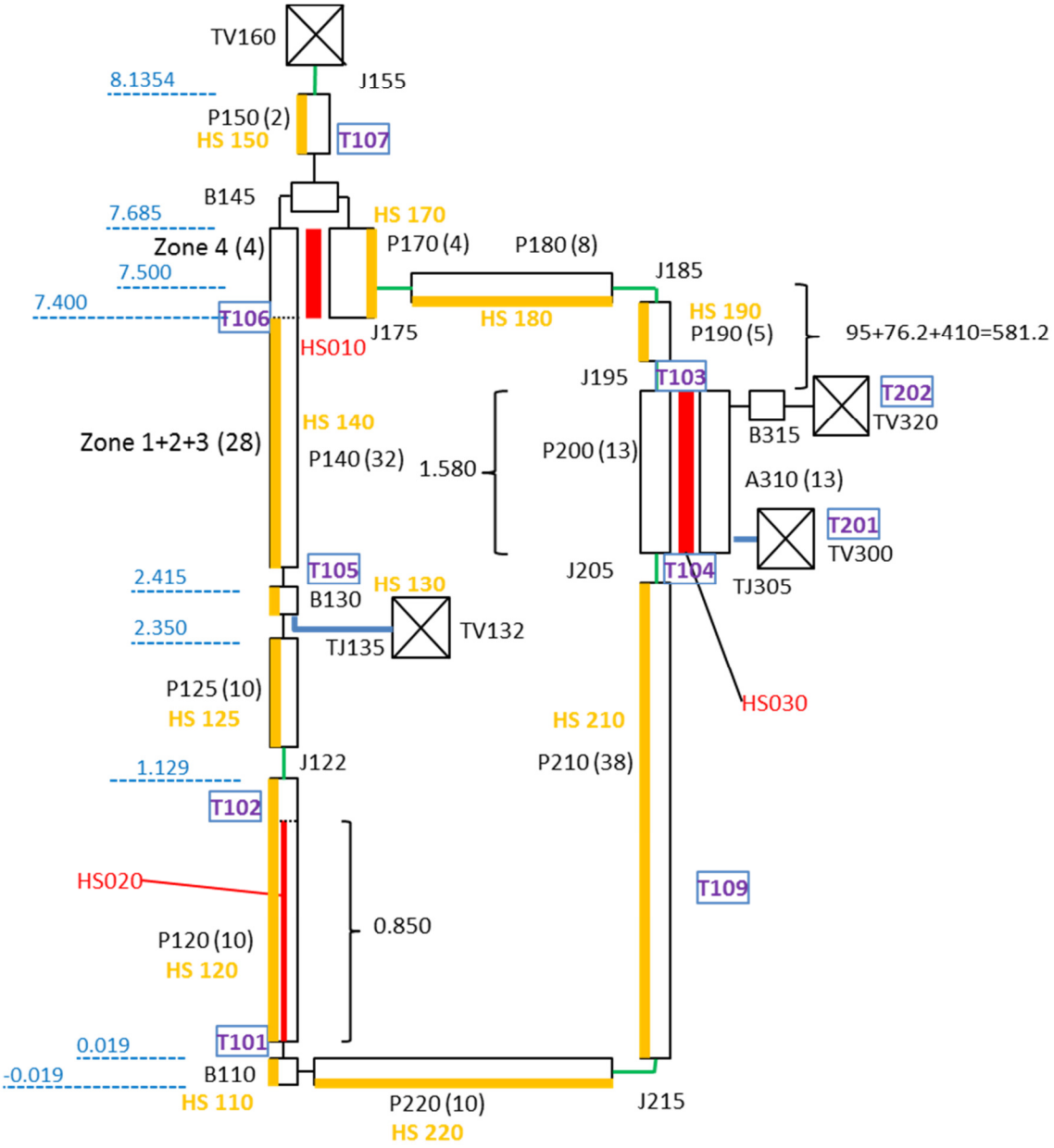

Figure 9 – Sketch of the 1D RELAP nodalization for NACIE loop.

Heat structures (HS) are then defined to account for the following heat transfers:

a) 010: Top of the riser → the annular part of the expansion vessel.

b) 020: FPS → LBE.

c) 030: LBE → water (heat exchanger).

- This HS is critical, because the series of heat resistances (convection and conduction) and the heat capacities of the various materials have a strong impact on the heat exchanger performance and on the system transient behaviour. The unavailability of accurate data makes it necessary to perform some tuning (e.g. on the thermal conductivity of the steel powder, which is initially guessed as 1/10 of the theoretical value for the steel).

d) 110 – 220: Heat losses to the atmosphere

- There HSs are also critical, because the heat losses are (especially on this facility) relatively large compared to the FPS and heat exchanger power (and can be seen by analysing the

measured data on LBE and water), and difficult to characterize. Again, some tuning is necessary to fit the measurements.

3.2 Boundary and initial conditions

Boundary conditions in terms of FPS power, water flow rate and water inlet temperature are shown in Figure 10, Figure 11 and Figure 12 respectively.

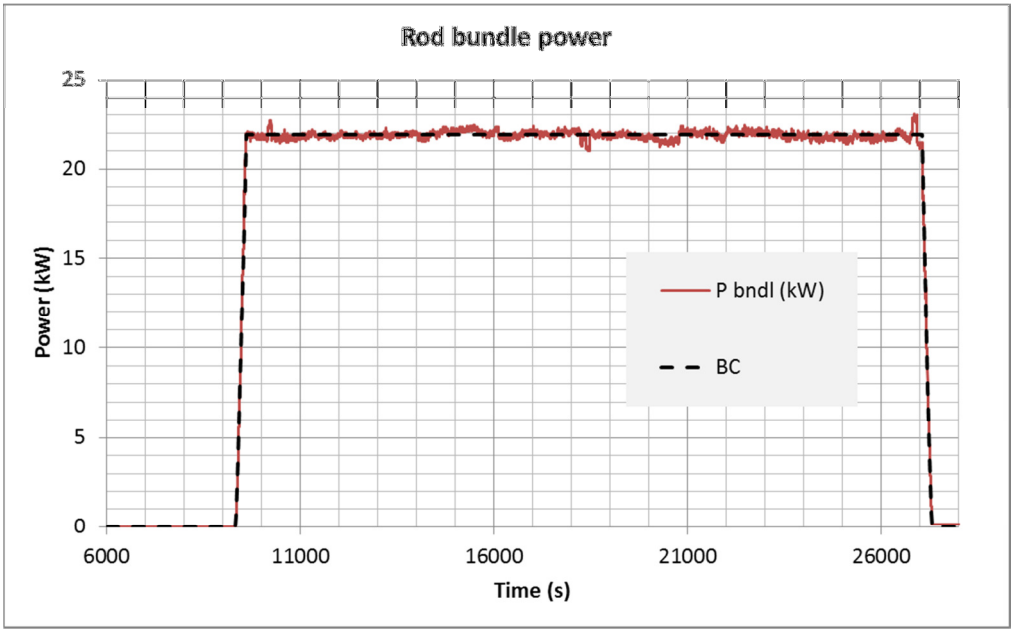

Figure 10 – Power BC.

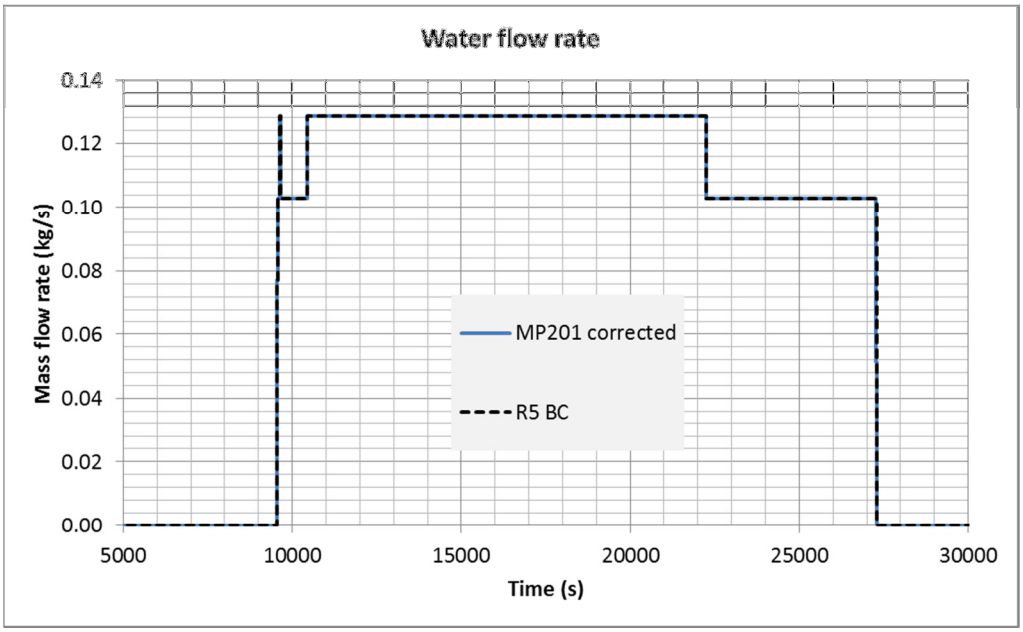

Figure 11 – Water flow rate BC.

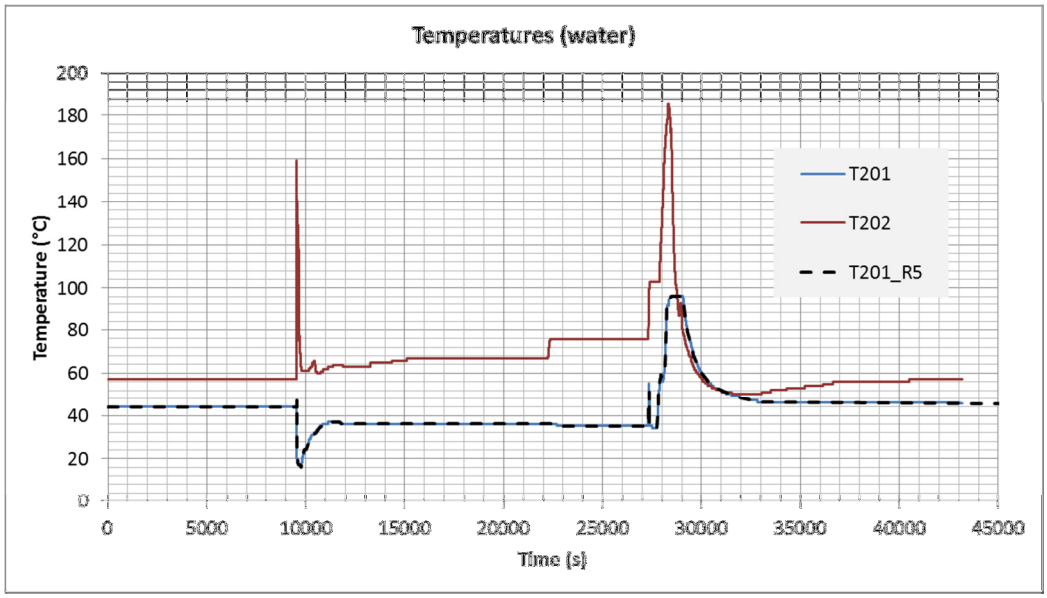

Figure 12 – Water inlet temperature BC.

Other boundary conditions:

- Water at HX outlet is at atmospheric pressure
- LBE expansion tank is at atmospheric pressure
- For the heat structures simulating the heat losses, a thermal boundary condition of the third type is used (ambient air temperature and free convection heat transfer coefficient, 10 W/m2/K)
    - The ambient temperature is specified through a table, and is not constant, see below

As regards the initial conditions:

- No LBE flow
- No water flow
- LBE temperature is set to 562 K everywhere
- Ambient temperature is initially set to 550 K, in order to take somehow into account the effect of the heating wires before the start of the power ramp; then the temperature is set to 283 K

The calculation is started at 9320 s, i.e. when the power ramp starts. No initialization calculation is run in order to avoid possible spurious LBE flows induced by numerical errors associated with the uncertainties in initial conditions from the experiment.

3.3 Post-test simulation results

Results of the post-test simulation of experiment no. 301 by the RELAP5-3D standalone model are shown in Figure 13 and Figure 14, in terms of LBE mass flow rate and water outlet temperature.

The predicted LBE flow rate accurately matches the experimental trend (better to say: the data obtained by the thermal balance). This also results from an appropriate characterization of the pressure drops along the circuit (particularly those due to the FPS spacer grids).

The temperature of water flowing out of the heat exchanger is predicted with satisfactory accuracy. This confirms also the appropriate characterization of heat losses.

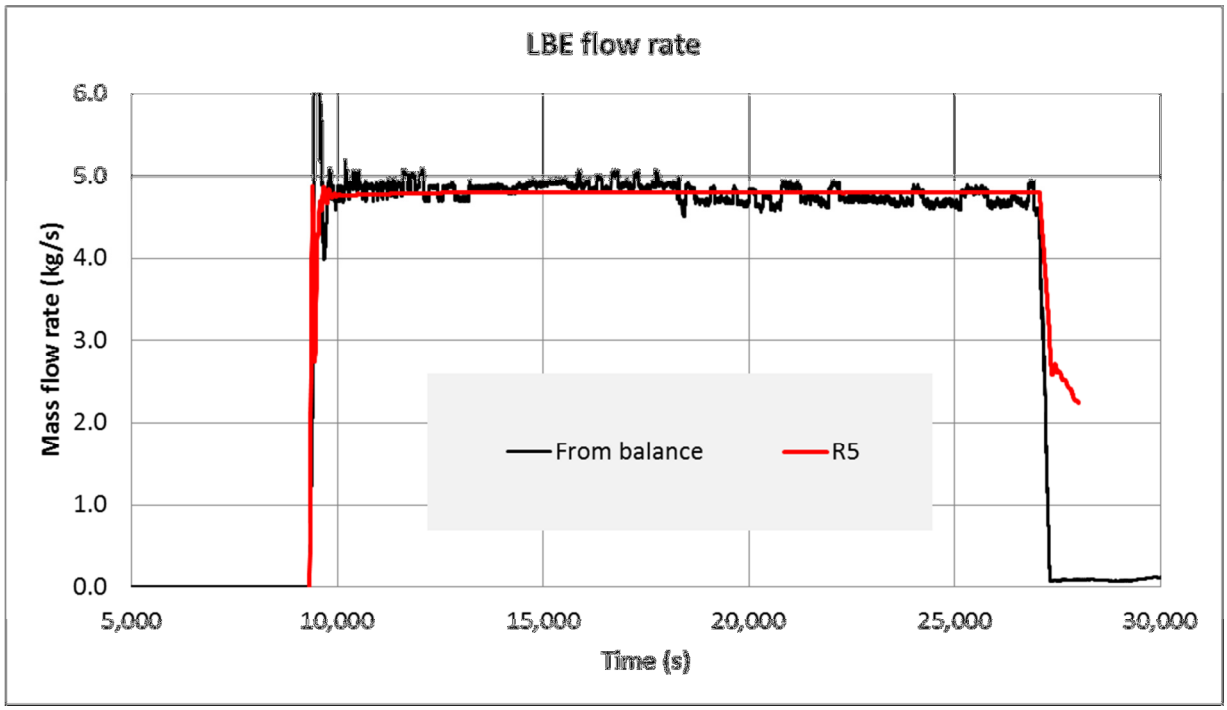

Figure 13 – RELAP results: LBE flow rate.

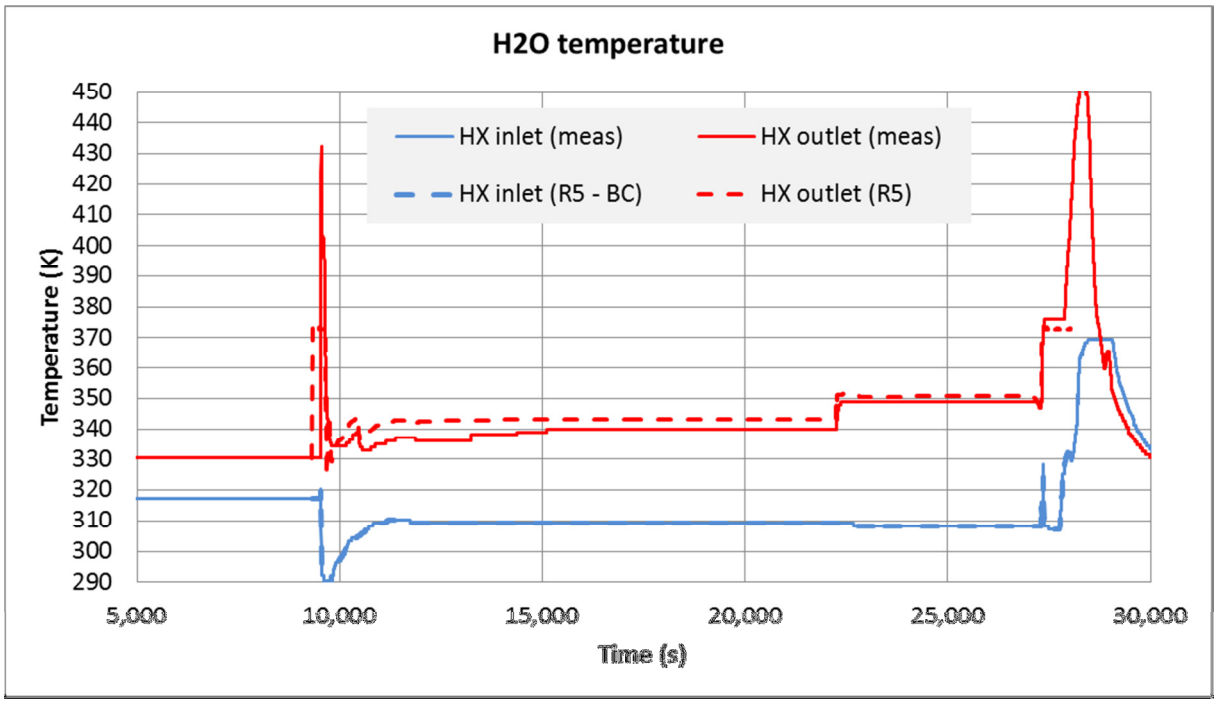

Figure 14 – RELAP results: water temperature.

4 CFX Model of the Heating Section

4.1 Computational Domain

The geometry taken into account for the development of the CFX standalone model of the heating section is composed of the following elements:

1. Tee-junction
2. Hot pin
3. Cold pin
4. Spacer bar
5. Spacer grid at the middle of the pins (modelled by a momentum sink)
6. Spacer grid at the top of the pins (simplified geometry included)
7. A part of the vertical tube (about 1 m), from the Tee junction up to 100 mm above the pin ending

In order to reduce the computational nodes, the symmetry over a vertical plane (plane XZ: identified by the axes of the vertical and horizontal parts of the piping included in the model) was used.

Figure 15 shows the overall domain. The hot pin is coloured in red, the cold pin in blue, the spacer bar in green and the old spacer grid in violet.

A detail of the top spacer grid geometry is shown in Figure 16.

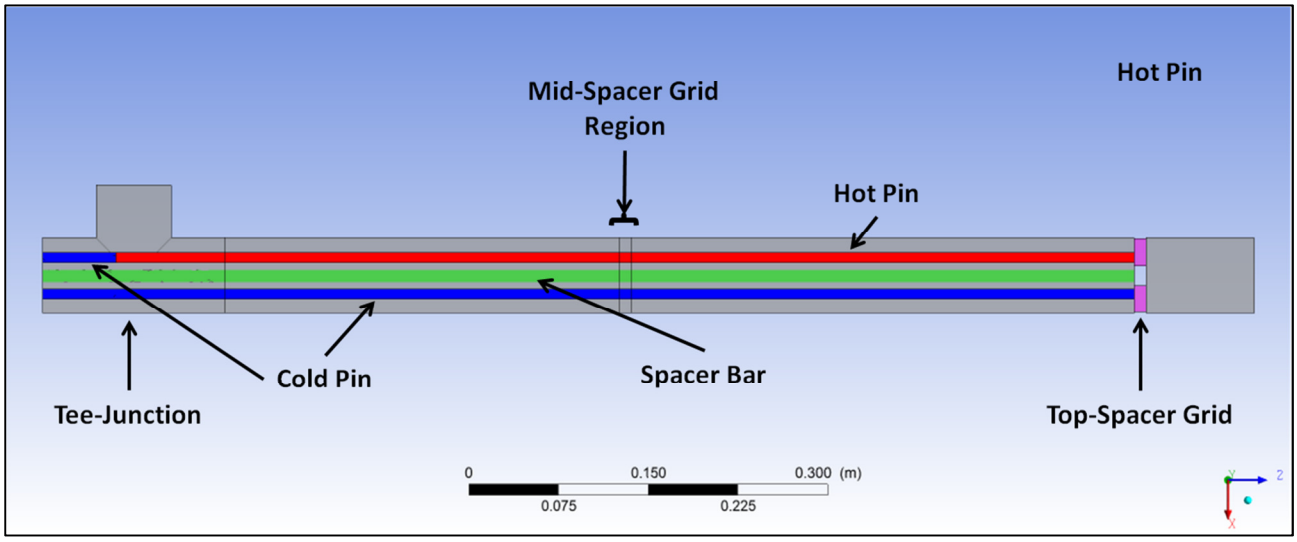

Figure 15 – CFX-standalone Computational Domain.

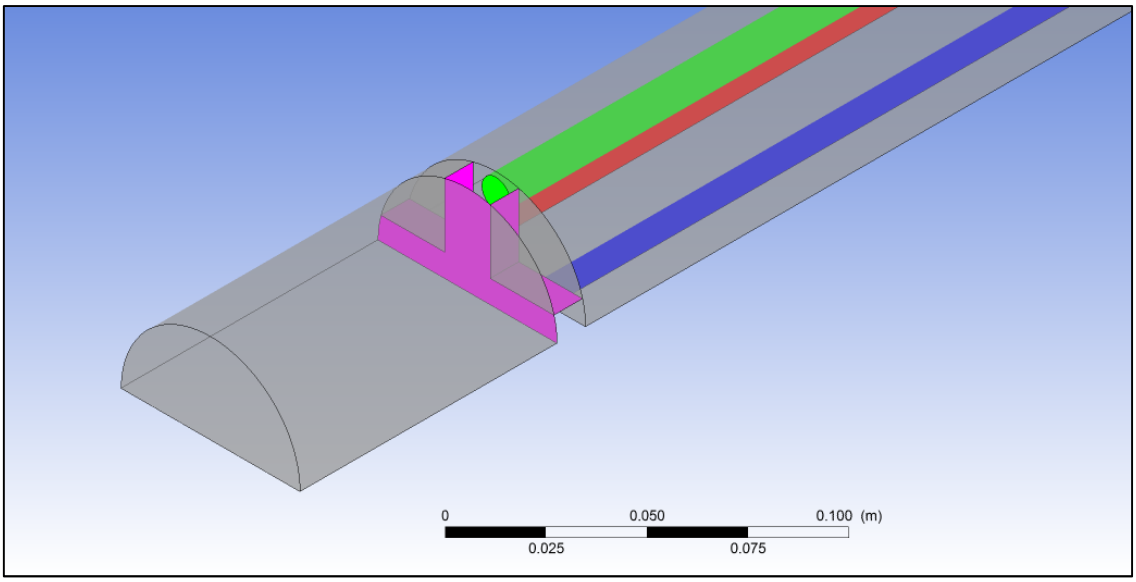

Figure 16 – CFX-standalone Computational Domain – Top-Spacer Grid.

4.2 Computational Grid

The developed grid consists mainly of two parts: a tetrahedral grid with prism layers near the walls for the Tee-junction region and an extruded prismatic grid for the vertical tube region above the T-junction. The Tee-junction grid has an overall ICEM quality above 0.3 and the first node from walls is at 0.5 mm (1 layer). The prismatic region has an overall quality above 0.55 and the first node from walls is at 0.1 mm for the pins (5 layers) and 0.5 mm for the remaining wall structures (spacer bar and outer tube, 1 layer). The surface grids at the interfaces between the tetrahedral and prismatic regions are not identical and a GGI interface was required. The total number of computational nodes is around 100 000.

The main features of the developed grids are shown from Figure 17 to Figure 19.

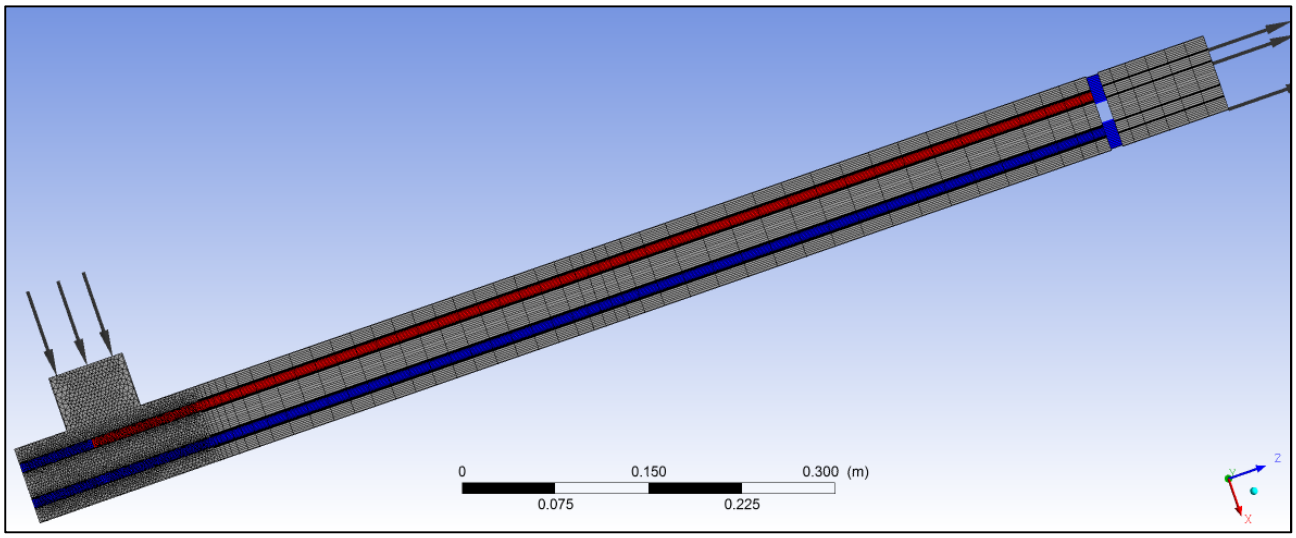

Figure 17 – CFX-standalone Computational Grid – Overall View.

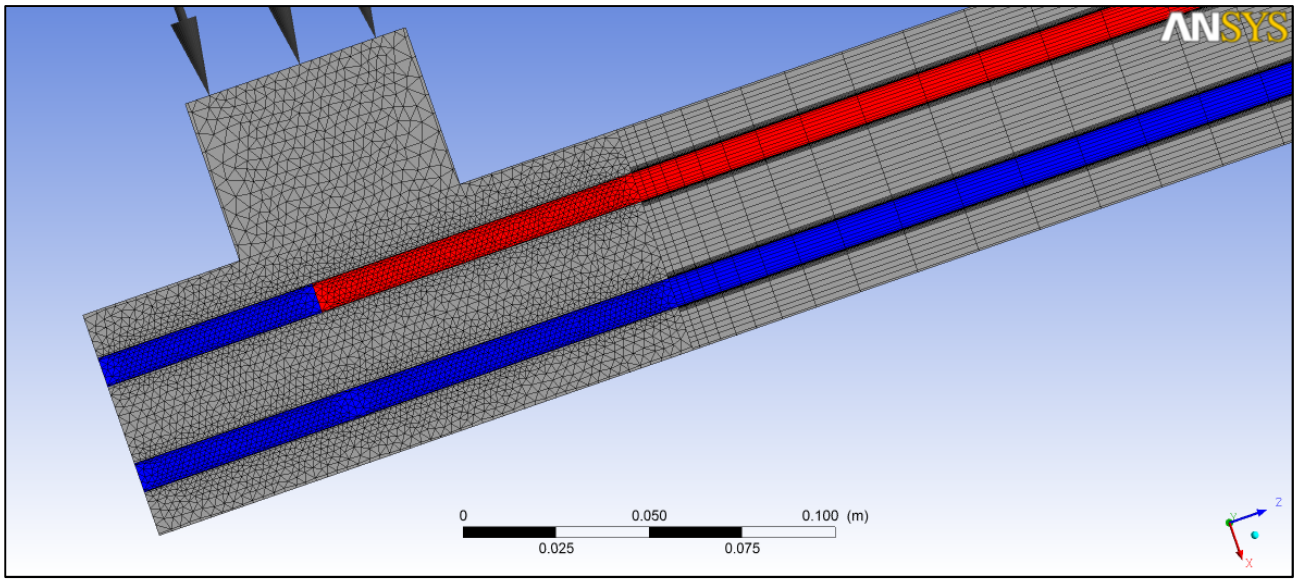

Figure 18 – CFX-standalone Computational Grid – Tee-Junction Detail.

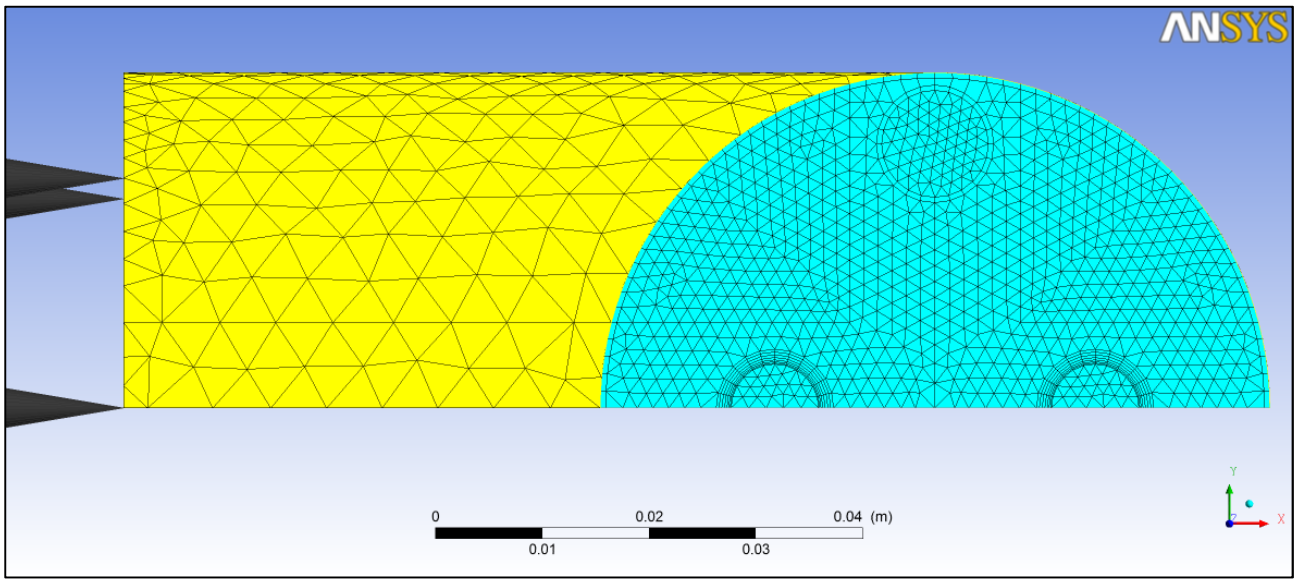

Figure 19 – CFX-standalone Computational Grid – 2D surface Grid at the Outlet.

4.3 Simulation Set-up

In order to test the developed CFX model, a standalone calculation was set up with the nominal flow rate of NACIE experiment no. 301. In particular, a mass flow of 4.9 kg/s was imposed at the Tee-Junction inlet. The hot pin heat flux was set to 100 W/cm^2 and an opening condition with zero relative pressure was imposed at the top boundary. A symmetric condition was imposed at the symmetry plane and all walls were considered as smooth.

The Mid-Spacer was modeled with a momentum loss region while flow around the top one can be directly solved (simplified geometry included in the computational domain).

Suitable properties of the working fluid (LBE) were imported in the code using properties tables generated from correlations taken from Ref. [12].

4.4 CFX-Standalone Results

Figure 20 shows the average temperature at the outlet boundary (100 mm above the pin end). A value of about 32 °C above the inlet value is obtained, which is in line with the results from the experiments and the RELAP standalone model.

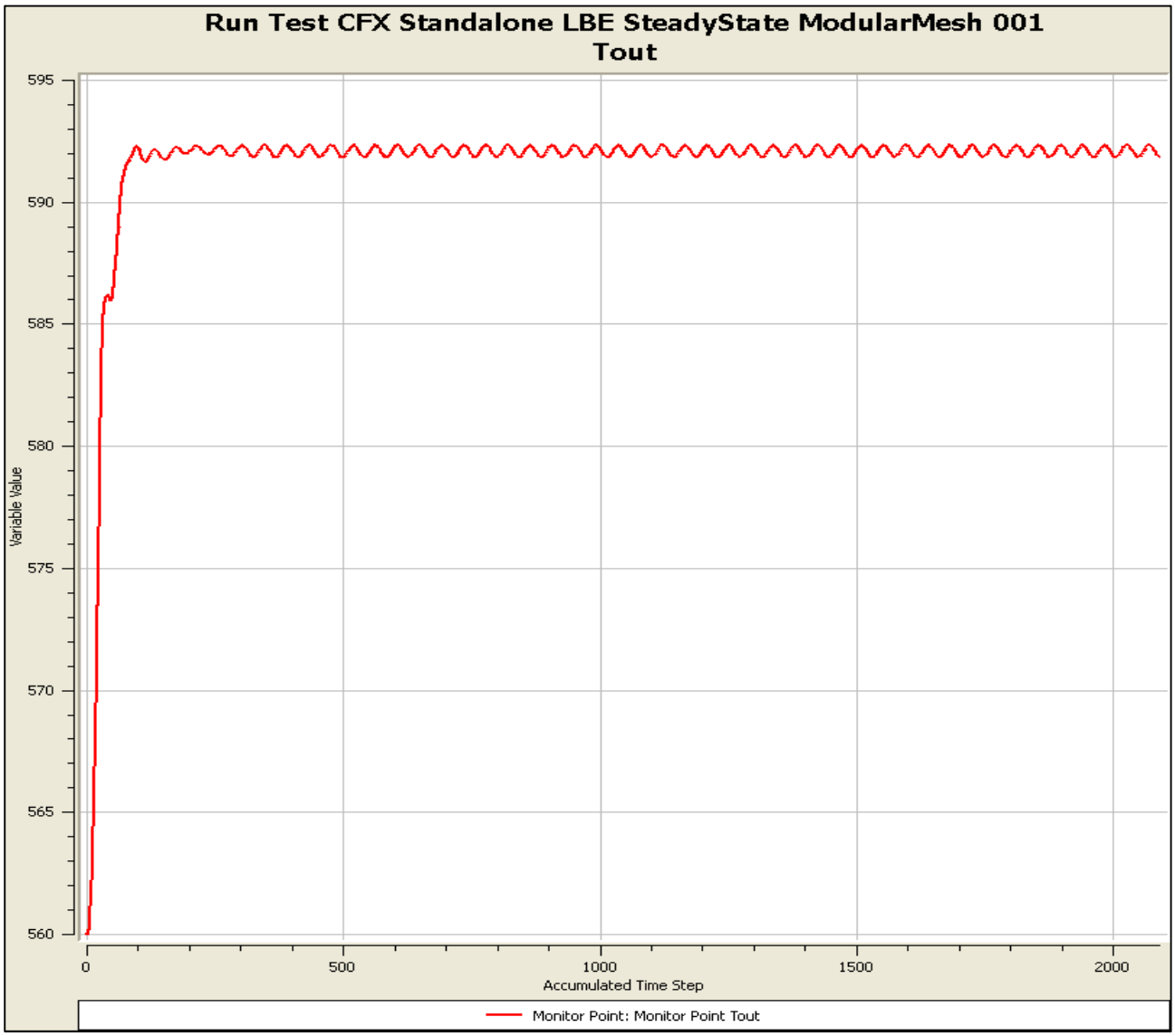

Figure 20 – Average Temperature at the Outlet Boundary.

The streamlines of velocity are shown in Figure 21, The increase in velocity after the Top-Spacer is clearly visible. It is worth noting that in the region just downstream the Tee-Junction, a circulation region is formed near the hot pin, where small or even negative velocities (with negative component in the z direction) can be identified (as shown in Figure 22 and Figure 23).

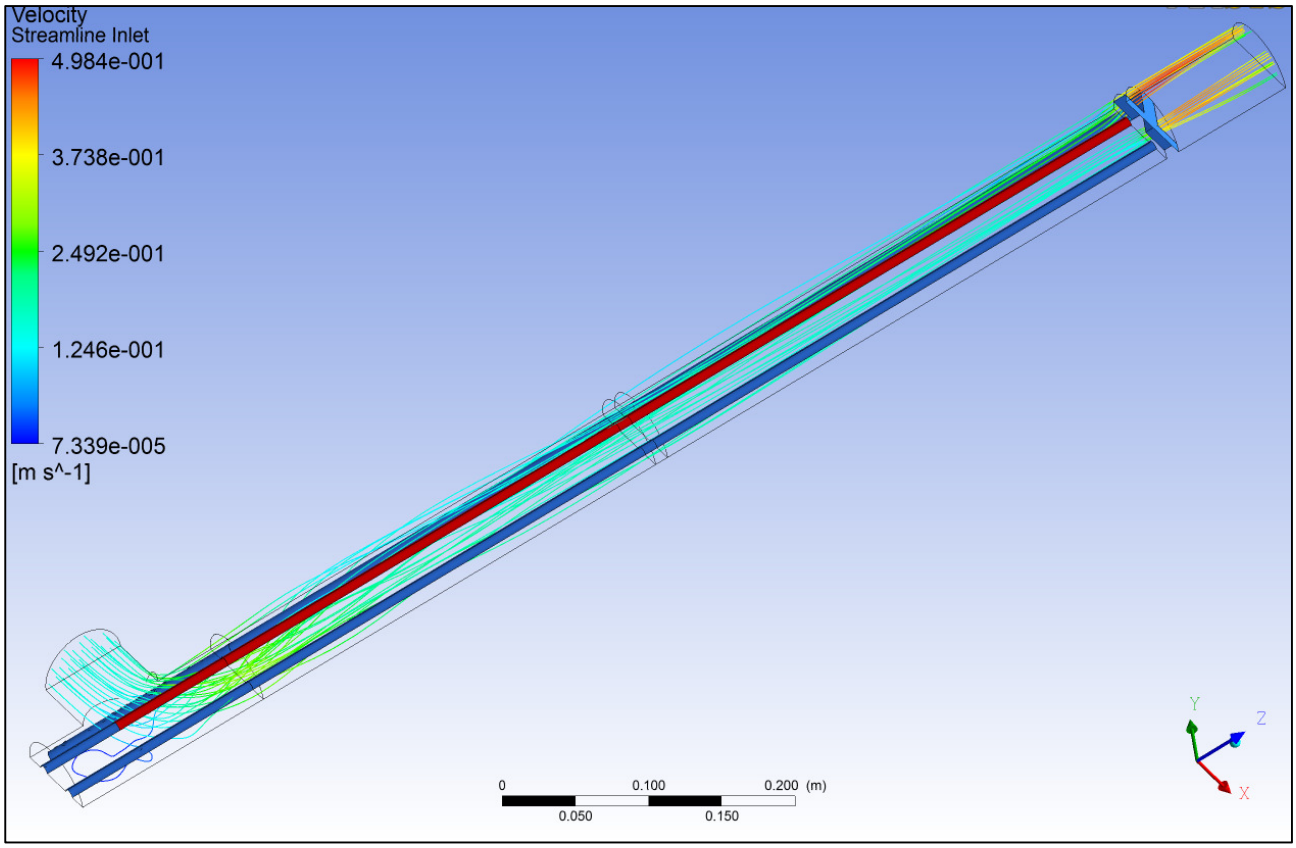

Figure 21 – Velocity Streamlines.

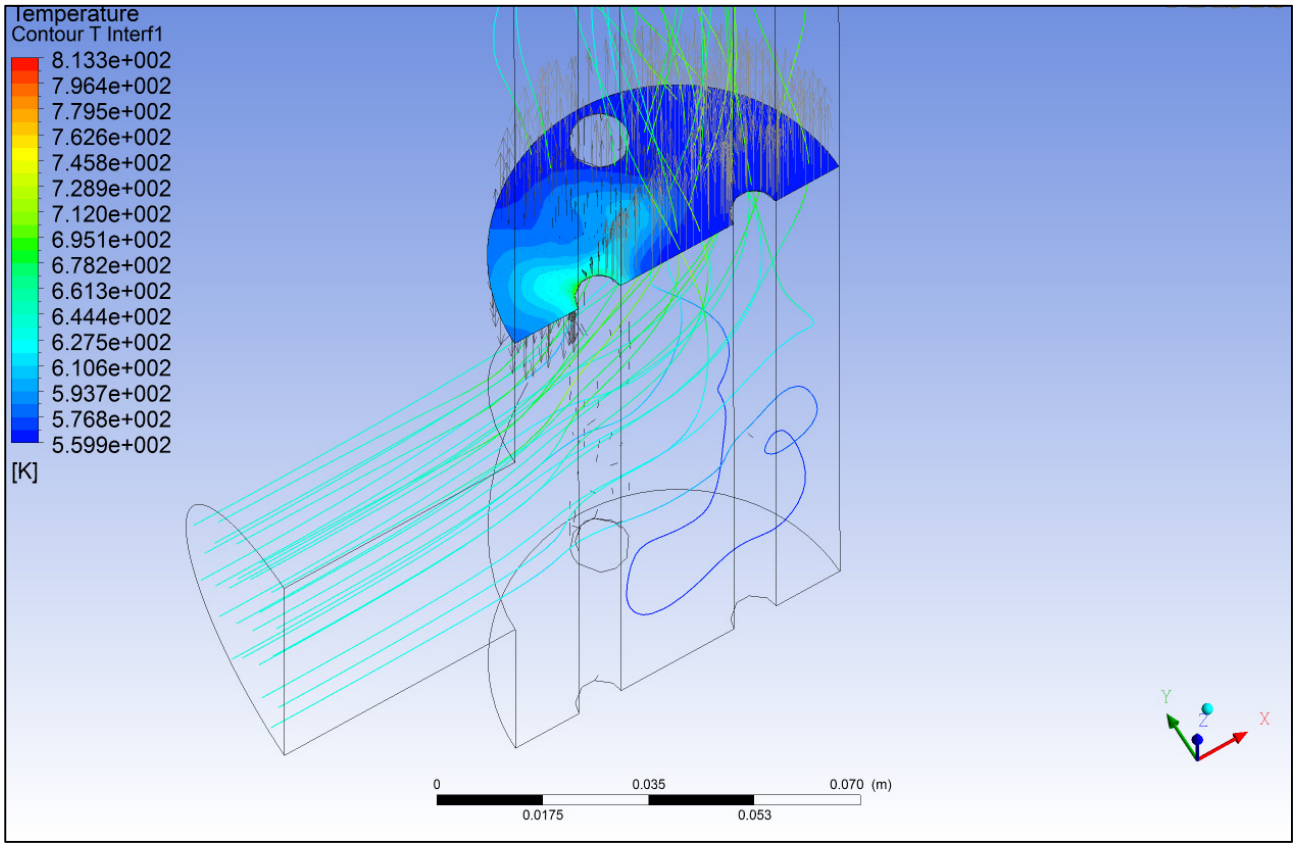

Figure 22 – Velocity Vectors and Temperature Contour Downstream the Tee-Junction.

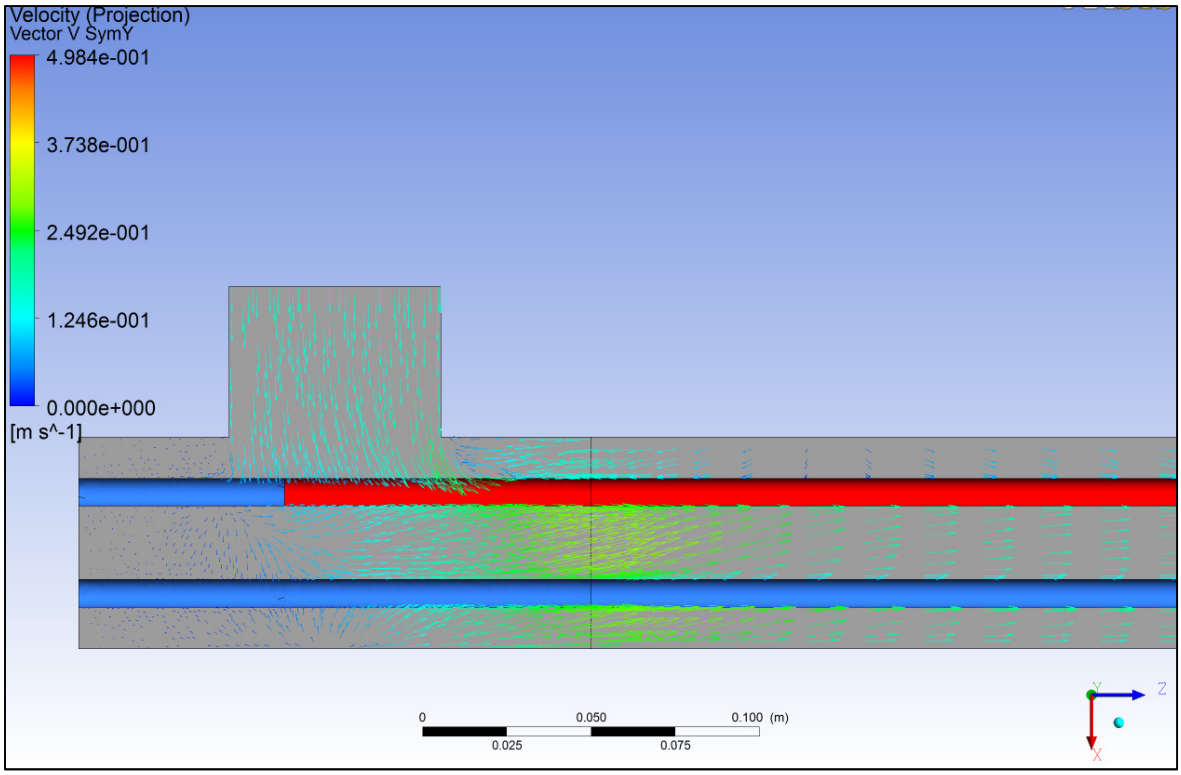

Figure 23 – Velocity Vectors at the Symmetry Plane Downstream the Tee-Junction.

Temperature Contours at different planes (z=100mm, z=300mm, z=500mm, z=700mm, Outlet Plane) are shown in Figure 24 below. It can be noted that the temperature distribution is still non-uniform at the Outlet boundary.

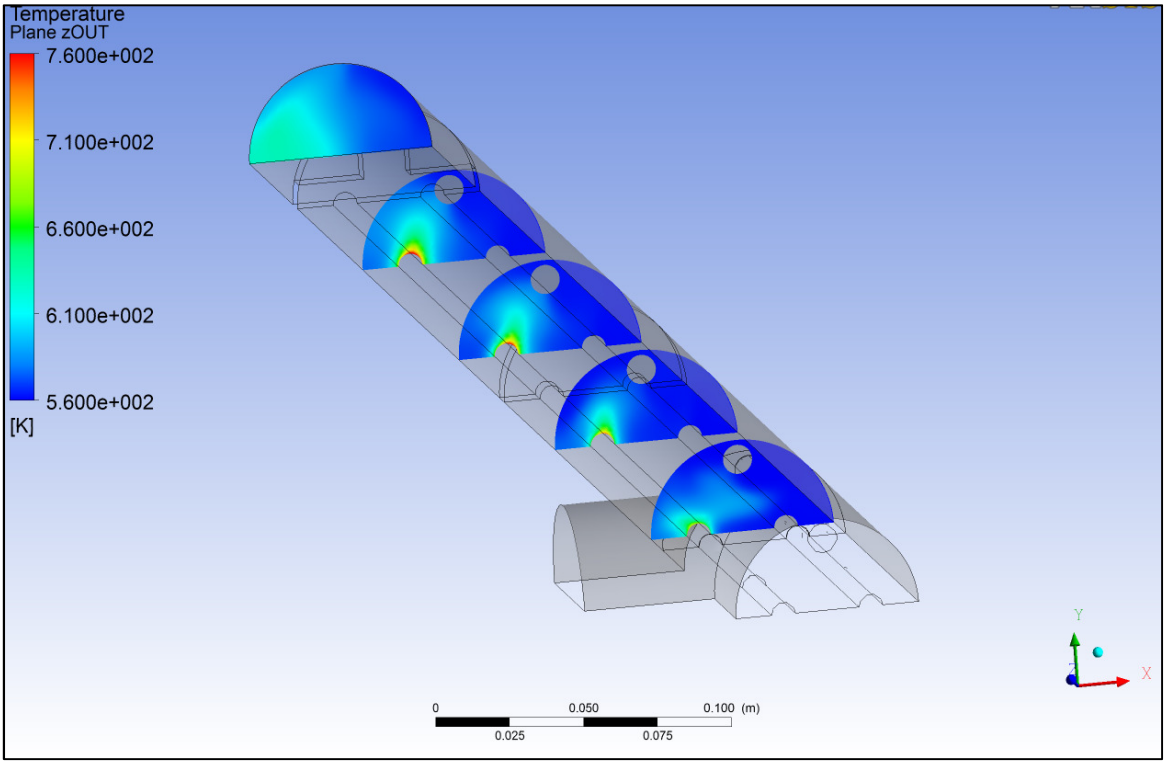

Figure 24 – Temperature Contours at Different Positions.

5 Coupled-code Analysis

The coupling between the SYS-TH code and CFD code follows the approach described in Refs. [2] and [3].

Static pressure, fluid temperature and fluid velocity are exchanged with a selected frequency at the inlet and outlet interfaces between the two calculation domains. Picture 25 depict the coupling flow chart.

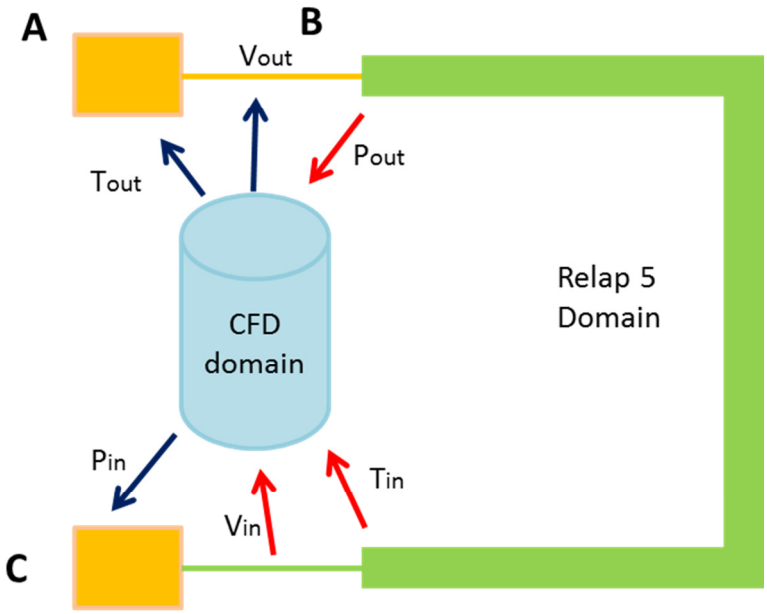

Figure 25 – Simplified sketch of the coupling procedure.

The RELAP5 calculation domain (in green) is modified by adding two TIME DEPENDENT VOLUME components (A and B in yellow) and a TIME DEPENDENT JUNCTION component (B in yellow). Those components are used to exchange the outlet temperature, outlet velocity and the inlet pressure from CFD domain to Relap5 (blue arrows).

The data exchange is managed by the coupling software that provides, at each coupling time, the CONTROL VARIABLES to set in the time dependent components the desired values.

Inlet velocity, inlet temperature and outlet pressure (red arrows) are passed from Relap5 domain to the CFD domain by the coupling software reading the correspondent values in the Relap5 output file. The coupling software adds in the original input deck the MINOR EDIT request cars for this purpose.

6 Conclusions and Future Development

The performed activity consisted in the application of the RELAP/CFX coupling tool, developed in the framework of previous PARs, to the simulation of one of NACIE natural circulation tests, with the objective of benchmarking the coupled-code tool and contributing to its qualification in view of the possible application to the analysis of nuclear reactor coolant systems.

The benchmarking demonstrated the applicability of the coupling tool to coolant systems involving natural circulation flows; the accurate description that the CFD models can provide of the detailed, three-dimensional, local flow and heat transfer phenomena, complements and enhances the system code capability to reliably describe the phenomena occurring at the loop-scale.

Further work may be envisaged in order to deepen the qualification of the coupling tool, extend its capabilities (e.g. to multi-phase and multi-component flows, etc.), and improve its numerical performance.

References

[1] ENEA e Ministero dello Sviluppo Economico, Accordo di Programma sulla Ricerca di Sistema Elettrico, Piano Annuale di Realizzazione (PAR) 2013, Gennaio 2014.

[2] L. Mengali, M. Lanfredini, F. Moretti, F. D'Auria, Stato dell'arte sull'accoppiamento fra codici di sistema e di fluidodinamica computazionale. Applicazione generale su sistemi a metallo liquido pesante, CIRTEN – Università di Pisa – Gruppo di Ricerca Nucleare di San Piero a Grado (GRNSPG), Report RdS/2012/1509, 31 Luglio 2012 – Versione 0, CERSE-UNIPI RL 1509/2011, Lavoro svolto in esecuzione dell'Attività LP3-C1.C AdP MSE-ENEA sulla Ricerca di Sistema Elettrico - PAR 2011.

[3] L. Mengali, M. Lanfredini, F. Moretti, F. D'Auria, Accoppiamento di codici CFD e codici di sistema, CIRTEN – Università di Pisa – Gruppo di Ricerca Nucleare di San Piero a Grado (GRNSPG), Report RdS/2013/048, 6 Settembre 2013 – Versione 0, CERSE-UNIPI RL 1510/2013, Lavoro svolto in esecuzione dell'Attività LP2-C1_d Progetto B.3.1 - AdP MSE-ENEA sulla Ricerca di Sistema Elettrico - PAR 2012.

[4] M. Polidori, P. Meloni, NACIE Benchmark Specifications and Experimental Data (LACANES) - Task Guideline for Phase 3: Characterization of NACIE (draft)

[5] ANSYS CFX-14.0 User Manual, 2012 (embedded in the software package).

[6] Idaho National Laboratories, RELAP5-3D Code Manuals, Appendix A – RELAP5-3D Input Data Requirements (version 4.0), INEEL-EXT-98-00834-V2, March 2012 (downloadable from http://www.inl.gov/relap5/r5manuals.htm)

[7] http://www.microsoft.com/visualstudio/ita/products/visual-studio-2010-express

[8] http://www.microsoft.com/it-it/download/details.aspx?id=17718

[9] ANSYS CFX-14.0 User Manual, 2012 (embedded in the software package).

[10] D. Wilcox, Turbulence Modelling for CFD, DCW Industries, Inc., Griffin printing, California, (2000).

[11] F. Menter, CFD Best Practice Guidelines for CFD Code Validation for Reactor-Safety Applications, EU/FP5 ECORA Project "Evaluation of computational fluid dynamic methods for reactor safety analysis", EVOL-ECORA-D01, Germany, February (2002).

[12] OECD/NEA Nuclear Science Committee, Handbook on Lead-bismuth Eutectic Alloy and Lead Properties, Materials Compatibility, Thermal-hydraulics and Technologies. OECD 2007, NEA No. 6195.

Curriculum Scientifico del Gruppo di Lavoro

Francesco D'auria

Professore Ordinario di Termoidraulica e di Ingegneria del Nocciolo (Moduli dell'insegnamento Termoidraulica e Ingegneria del Nocciolo Cod. 424II) per il Corso di Laurea Magistrale in Ingegneria Nucleare - Università di Pisa.

Autore di oltre 100 articoli su rivista e numerose altre pubblicazioni.

(http://arp.unipi.it/listedoc.php?ide=5808).

Marco Lanfredini

Laureando in Ingegneria Nucleare, collaboratore dal 2011 presso il Gruppo di Ricerca Nucleare S. Piero a Grado - Università di Pisa quale utilizzatore di codici termoidraulici di sistema.

Autore di rapporti tecnici interni e di articoli scientifici facilmente reperibili sui principali motori di ricerca specializzati.

Lorenzo Mengali

Ingegnere Aerospaziale, collaboratore dal 2008 presso il Gruppo di Ricerca Nucleare S. Piero a Grado - Università di Pisa, quale esperto di Fluidodinamica Computazionale.

Autore di rapporti tecnici interni e di articoli scientifici facilmente reperibili sui principali motori di ricerca specializzati.

Fabio Moretti

Ingegnere Nucleare (2004), Dottore di Ricerca in Sicurezza Nucleare e Industriale (2009), collaboratore dal 2008 presso il Gruppo di Ricerca Nucleare S. Piero a Grado - Università di Pisa, quale coordinatore dell'area Fluidodinamica Computazionale e responsabile di attività sperimentali e di training.

Autore di rapporti tecnici interni e di articoli scientifici facilmente reperibili sui principali motori di ricerca specializzati.